Chemosphere 390 (2025) 144718

Contents lists available at ScienceDirect

Chemosphere

journal homepage: www.elsevier.com/locate/chemosphere

Iron-mediated protein–humic acid interactions under aerobic and anaerobic conditions: Implications for protein hydrolysis and wastewater treatment

Muhammad Fauzul Imron [a,b,*], Lenno van den Berg [c], Alexander T.W.M. Hendriks [c], Ralph E.F. Lindeboom [a], Merle K. de Kreuk [a]

[a] Section of Sanitary Engineering, Department of Water Management, Faculty of Civil Engineering and Geosciences, Delft University of Technology, Stevinweg 1, Delft, 2628CN, The Netherlands
[b] Study Program of Environmental Engineering, Department of Biology, Faculty of Science and Technology, Universitas Airlangga, Kampus C UNAIR, Jalan Mulyorejo, Surabaya, 60115, Indonesia
[c] Haskoning, Laan 1914 no 35, Amersfoort, 3818EX, The Netherlands

HIGHLIGHTS

- Iron affects protein-HA complexation under different redox states.
- Fe(III)-protein-HA complexes inhibit protein hydrolysis >90 % aerobically.
- Binding involves electrostatic and coordination interactions.
- Reducing Fe(III) to Fe(II) leads to smaller and less stable complexes.

GRAPHICAL ABSTRACT

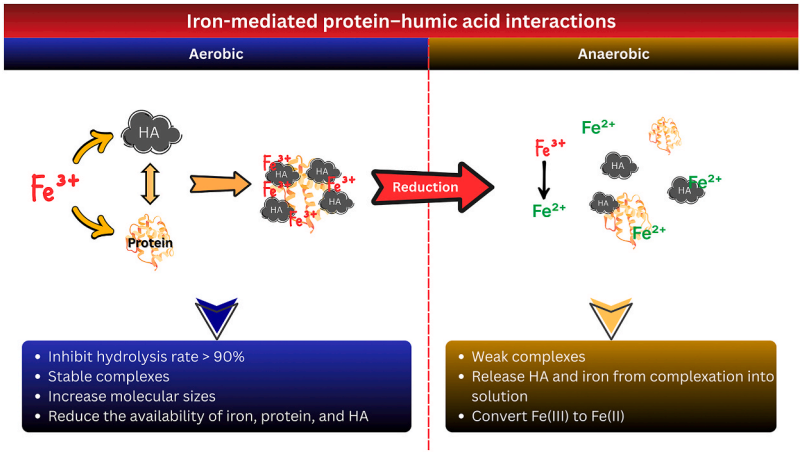

ARTICLE INFO

Handling Editor name: Paolo Roccaro

Keywords:
Degradation rate
Iron complexation
Organic compounds

ABSTRACT

Proteins and carbohydrates are both major biodegradable fractions in wastewater. Complexation with coexisting compounds, such as iron (Fe) and humic acids (HA), which are both commonly present in wastewater, could influence the different degradation rates of proteins and carbohydrates. Depending on the redox conditions, Fe exists as Fe(II) or Fe(III), with differing binding affinities and chemical behaviour. This research aims to systematically assess the complex interaction between Fe, protein, and HA compounds under aerobic and anaerobic conditions. The results showed that the addition of Fe(III) and HA to a protein solution inhibited its hydrolysis

* Corresponding author. Section of Sanitary Engineering, Department of Water Management, Faculty of Civil Engineering and Geosciences, Delft University of Technology, Stevinweg 1, Delft, 2628CN, The Netherlands.
E-mail addresses: M.F.Imron@tudelft.nl (M.F. Imron), M.K.deKreuk@tudelft.nl (M.K. de Kreuk).

https://doi.org/10.1016/j.chemosphere.2025.144718
Received 23 June 2025; Received in revised form 20 September 2025; Accepted 3 October 2025
Available online 11 October 2025

Pollutants
Wastewater treatment

rate by more than 90 % under aerobic conditions. In contrast, interactions between the same compounds and carbohydrates were much weaker and had a minimal effect on hydrolysis rates. Complexation with Fe, proteins, and HA was indicated by increased molecular sizes and reduced concentrations of free iron, protein, and HA. FTIR results showed that Fe(III) formed complexes with proteins and HA through electrostatic and coordination bonds involving various functional groups. Anaerobic reduction of Fe(III) to Fe(II) by hydrazine resulted in weaker binding and the formation of smaller, less stable protein–humic acid complexes. These findings suggested that modulating Fe complexation under alternating aerobic and anaerobic conditions, such as those found in redox-cycling wastewater treatment, can be a promising strategy to enhance protein degradation.

1. Introduction

Proteins and carbohydrates are among the major organic compounds present in wastewater (Mbamalu Ezeh et al., 2024). These compounds differ in degradation behaviour: carbohydrates tend to degrade more quickly and easily than proteins (Yang et al., 2015). In addition, HA, which are also commonly found in wastewater, are known to interact with proteins and carbohydrates, forming complex compounds (Fernandes et al., 2015; Zhu et al., 2023). Such complexation can affect the degradation efficiency during treatment processes (Aiken et al., 2011). Iron (Fe) is frequently added in wastewater treatment to precipitate phosphorus. However, this addition also promotes aggregation of organic compounds, facilitating their removal from wastewater through phase separation (Knap-Bałdyga and Żubrowska-Sudoł, 2023; Qasem et al., 2021).

Mundra et al. (2023) reported different properties of Fe during aerobic and anaerobic processes in wastewater treatment. Under aerated conditions, Fe mainly exists as Fe(III), which can form stable complexes with organic molecules through charge neutralization and electrostatic bridging of functional groups (Kurniawan et al., 2023; Zhu et al., 2011). However, under anaerobic conditions, Fe(III) is reduced to Fe(II), which destabilizes the equilibria of these complexes and could release (part of) its bound organic matter (Chen et al., 2018). Iron-reducing bacteria reduce Fe(III) under anaerobic conditions, leading to a reduced complexation of waste-activated sludge (WAS), causing the disintegration of its sludge flocs and the dissolution of organic compounds (Zhan et al., 2021). Nevertheless, both Fe(III) and Fe(II) complexes with HA are water-stable (Catrouillet et al., 2014; Fujii et al., 2014), while Fe(III) competes favourably for the most stable binding sites (Steinhauser et al., 2004). Due to its higher positive charge, Fe(III) is a stronger Lewis acid than Fe(II), which results in the formation of more stable complexes (Maity et al., 2019).

The interaction of Fe with organic matter, specifically with HA, has been widely reported. Kügler et al. (2019) found that the interaction of Fe with organic matter in aquatic environments can prevent the decomposition of organic matter. Fe-HA complexes have a large effect on the transformation and migration of organic matter, affecting the availability of the organic matter (Di Iorio et al., 2022). The same finding was reported by X. Li et al. (2020), who observed that iron cations are capable of interacting with the carboxyl, phenolic, and hydroxyl functional groups of humic acid to form stable Fe-HA complexes. Interactions between Fe and proteins, as well as with carbohydrates, can play a significant role in wastewater treatment. Research by Mittal et al. (2015) showed that iron is a robust binder to proteins, forming Fe-protein complexes that elicit the availability of protein for degradation. Similarly, Pichtel et al. (1989) reported that Fe can agglomerate with carbohydrate via charge neutralization in wastewater. Although many studies have examined the complexation of Fe with organic compounds, those typically focus on an individual interaction, like Fe with HA, Fe with proteins, or Fe with carbohydrates; less is understood about how various organic compounds can affect each other's complexation properties. Furthermore, the effects of such complexation on hydrolysis efficiency and rates over a range of redox conditions have not been examined to the author's knowledge.

To bridge this gap, the goal of this study is to investigate the Fe binding to protein–HA complexes under aerobic and anaerobic conditions and the effect of Fe-protein-HA complexation on the protein hydrolysis rate. In addition, the study analysed how altering the oxidation state of Fe and/or adding reducing agents affected the Fe-protein-HA complexes under different redox conditions. Carbohydrate hydrolysis was examined separately as a reference to assess whether the inhibitory effects of Fe and HA were specific to proteins or also extended to other biodegradable fractions. The findings of this study can contribute to improved understanding of the role of Fe in relation to the redox conditions in wastewater treatment, which can then be used as a reference for improving wastewater treatment systems.

2. Materials and methods

2.1. Protein and carbohydrate hydrolysis rate analysis

Protease and cellulase activities were measured using the Pierce Fluorescent Protease Assay Kit (Thermo Fisher Scientific, USA) and the Fluorescent Cellulase Assay Kit (Marker Gene Technologies Inc., USA) to assess protein and carbohydrate hydrolysis rates, respectively. Experiments were conducted in 96-well plates (Corning Inc., 3603 Costar, USA) under both aerobic and anaerobic conditions. Control vessels contained single compounds, while mixed vessels contained compound mixtures. Two solutions were prepared: a sample solution with Fe, humic acid, and enzymes, and a substrate solution with protein and carbohydrate. FTC-Casein (protein) and Resorufin Cellobioside (carbohydrate), provided in the kit, served as the respective substrates. Each well was filled with 50 μL of sample and 50 μL of substrate. For anaerobic assays, samples were prepared in a glove bag (Cole-Parmer Instrument, USA) and flushed with nitrogen to maintain an oxygen-free environment. Plates were sealed with parafilm during measurement to preserve anaerobic conditions. For aerobic assays, plates remained uncovered.

Iron in this research was introduced as $FeCl_3.6H_2O$ (Sigma-Aldrich, USA) for aerobic conditions and $FeCl_2.4H_2O$ (Merck, Germany) for anaerobic conditions at concentrations of 5, 10, and 15 mg L^{-1}, representing low, medium, and high iron dosages, respectively. The concentrations of humic acid sodium salt (Sigma-Aldrich, Germany) used were 20, 40, and 60 mg L^{-1} to achieve protein/HA ratios of 0.5, 0.25, and 0.17 and carbohydrate/HA ratios of 0.4, 0.2, and 0.1. TPCK-Trypsin, as a protease, provided in the respective test kits, was used in the protein solution. At the same time, cellulase enzyme from *Aspergillus niger* (Sigma-Aldrich, USA) was used in the carbohydrate solution. The protein was prepared with a concentration of 0.01 mg mL^{-1} (0.00042 mM). While carbohydrate concentration was 0.008 mg mL^{-1} (0.015 mM). The concentrations of protein, carbohydrate, and HA in this research were determined based on the characteristics of wastewater at the Harnaschpolder wastewater treatment plant (WWTP) in the Netherlands, which is then varied with ratios above and below the average (Gonzalez et al., 2021).

Cellulase and protease activities were quantified by measuring fluorescence increases with a FLUOstar Galaxy Multi-functional Microplate Reader (BMG Technologies, UK) at excitation/emission wavelengths of 530/590 nm and 485/520 nm, respectively. Calibration curves were generated to determine the concentrations of the product.

The influence of Fe and HA on hydrolysis was evaluated using a first-order kinetic equation (Eq. (1)). Reaction time (t) was plotted on the x-axis and product concentration at time t on the y-axis to determine the rate constant (k). Curve fitting was conducted using MATLAB R2023b (MathWorks, USA). Product concentrations were calculated by correlating measured fluorescence (relative fluorescence units, RFU) to the calibration curve.

$$[A]_t = [A]_0 e^{-kt} \quad \text{Eq. (1)}$$

Where $[A]_t$ is the concentration at time t, and $[A]_0$ is the concentration at time 0, and k is the first-order rate constant.

Calculated hydrolysis rates were analysed using analysis of variance (ANOVA) to identify significant differences ($p \leq 0.05$) between factors such as Fe and HA concentrations in relation to the measured responses (Imron et al., 2023). All measurements were performed in triplicate.

2.2. Complexation analysis of protein and HA with Fe(III)

This experiment aimed to analyse the effect of Fe(III) on protein and HA complexation under different redox conditions. The focus was limited to physicochemical processes, excluding biological interactions. Bovine serum albumin (Sigma-Aldrich, Germany) and humic acid sodium salt (Sigma-Aldrich, Germany) were used as protein and HA stock, respectively. The protein and HA concentrations used were 36 ± 0.35 mg L^{-1} and 135 ± 0.23 mg L^{-1} for aerobic and anaerobic conditions, respectively, to obtain a protein/HA ratio similar to that in the hydrolysis experiment. In this experiment, 10 mg L^{-1} of Fe(III) was used under both redox conditions and 0.1 % of hydrazine, known as a reducing agent, was added under anaerobic conditions to promote the reduction process of Fe(III) to Fe(II) directly after aerobic conditions. To verify consistency, an additional experiment was conducted using 2.5 mg L^{-1} of Fe(III) under aerobic conditions and at 2.5 mg L^{-1} of Fe(II) under anaerobic.

The experiment was conducted using 100 mL Schott Duran bottles with seven different types of solutions, each with a total volume of 50 mL, containing the following components: Fe (control 1), protein (control 2), HA (control 3), protein + HA, Fe + protein, iron + HA, and Fe + protein + HA, for each condition both aerobic and anaerobic, with each condition maintained for 1 h. The samples were stirred using a magnetic stirrer (Labinco, The Netherlands) set to 10 % of rpm (max 1250 rpm). Furthermore, nitrogen gas was flushed into the bottle for around 5 min to maintain anaerobic conditions.

To determine the effect of different redox conditions, the concentrations of free Fe, protein, and HA were measured. Free Fe, protein, and HA refer to non-complexed molecules present in the liquid after filtration, measured against the controls. Additionally, the complexation of Fe with protein and HA was analysed using high-performance liquid chromatography (HPLC) (Prominence, Shimadzu, Japan).

2.3. SEC-HPLC analysis

Size exclusion-high performance liquid chromatography (SEC-HPLC) was performed to analyse the complexation of iron with protein and HA. Samples were collected after the aerobic and anaerobic processes and filtered using 10 ml syringe equipped with 0.45 μm CHROMAFIL Xtra PES-45/25 filter (Macherey-Nagel, Germany) to separate the complexed compounds from non-complexed molecules. The SEC-HPLC column used was a Yarra™ 3 μm SEC-2000 model (LC Column 300 × 7.8 mm, Ea; Phenomenex, USA) connected to an ultrafast liquid chromatography (UFLC) system (Prominence, Shimadzu, Japan).

Since the samples contained Fe, ammonium acetate (40 mM, pH 7) (Sigma-Aldrich, Germany) was used as the mobile phase to prevent precipitation. The eluent flow rate was set to 1 mL/min for 20 min at 35 °C. The SEC-HPLC detector was configured to operate at two wavelengths: 280 nm for protein detection and 254 nm for humic substance detection. The HPLC results were expressed as the area under the detector signal curve (in mV) over a time corresponding to the molecular weight of the measured compounds.

2.4. FTIR spectroscopy analysis

Fourier-transform infrared (FTIR) spectroscopy was employed to analyse the functional groups of protein and HA (Dampang et al., 2021). Prior to the FTIR analysis, samples from the aerobic conditions of the complexation experiments were prepared using a freeze-dryer (BioBase, China) to remove moisture, ensuring a stable and dry state for accurate measurement. Then, FTIR spectra of the samples were performed on an FTIR Spectrophotometer (PerkinElmer, Shelton, CT, USA) at room temperature with ATR mode, within a wavenumber range from 600 cm^{-1}–4000 cm^{-1}. A resolution of 2 cm^{-1} and an accumulation of 4 scans were applied to each sample.

2.5. Chemical analysis

The concentrations of free Fe, protein, and humic acid were measured as follows. Before being analysed, samples were filtered using a 10 mL syringe equipped with a 0.45 μm filter to separate the complexed compounds from non-complexed molecules. Free Fe concentration was analysed using the Hach kits LCK 320 (HACH, USA) and measured with the HACH DR3900 instrument (HACH, USA), representing the Fe(III) and Fe(II) concentration results. The free protein and humic acid concentrations were measured using the Lowry method, following adjustments for humic substance interference as described by Frølund et al. (1995). However, the Lowry method was applied only to measure protein and humic acid concentrations in the control sample under aerobic conditions. For anaerobic conditions, to avoid interference with the spectrophotometric measurements by hydrazine, protein and humic acid concentrations were determined by comparing the control and mix solution's surface area generated by HPLC.

3. Results and discussions

3.1. Hydrolysis rate of protein and carbohydrate

The results show that protein hydrolysis is highly susceptible to inhibition by Fe and HA, whereas carbohydrate hydrolysis is only slightly affected. As shown in Fig. 1a and b, the protein hydrolysis rate decreased by more than 50 % when only Fe(III) and/or Fe(II) was present (15 mg L^{-1}), and by more than 80–90 % when combined with high HA concentrations (60 mg L^{-1}). The protein/HA ratios tested here were comparable to those measured in the influent of the Harnaschpolder WWTP (27 mg L^{-1} protein and 105 mg L^{-1} HA), and thus support the relevance of the findings to operational wastewater treatment systems. (Gonzalez et al., 2021).

The likely mechanisms for this inhibition are electrostatic and coordination interactions, as evidenced in Section 3.3. The positively charged Fe, can bind strongly to the negatively charged carboxyl and phosphate groups of casein, decreasing its availability for degradation (Mittal et al., 2015). HA can additionally reduce enzymatic activity by interacting with positively charged amino groups in proteases such as trypsin, thereby altering enzyme flexibility, stability, and activity (Yap et al., 2018). Together, Fe and HA may form ternary complexes with proteins, further reducing hydrolysis efficiency.

By contrast, carbohydrate hydrolysis (Fig. 1c and d) was only mildly inhibited, even at the highest Fe or HA concentrations, with reductions below 10 %. Under aerobic conditions (Fig. 1c), 15 mg L^{-1} of Fe(III) reduced carbohydrate hydrolysis by less than 5 %, while HA alone caused some inhibition across all tested concentrations. This suggests that both Fe and HA can interfere with carbohydrate degradation, although the overall effect is much weaker than for proteins. Previous studies reported that Fe can form complexes with polysaccharides and

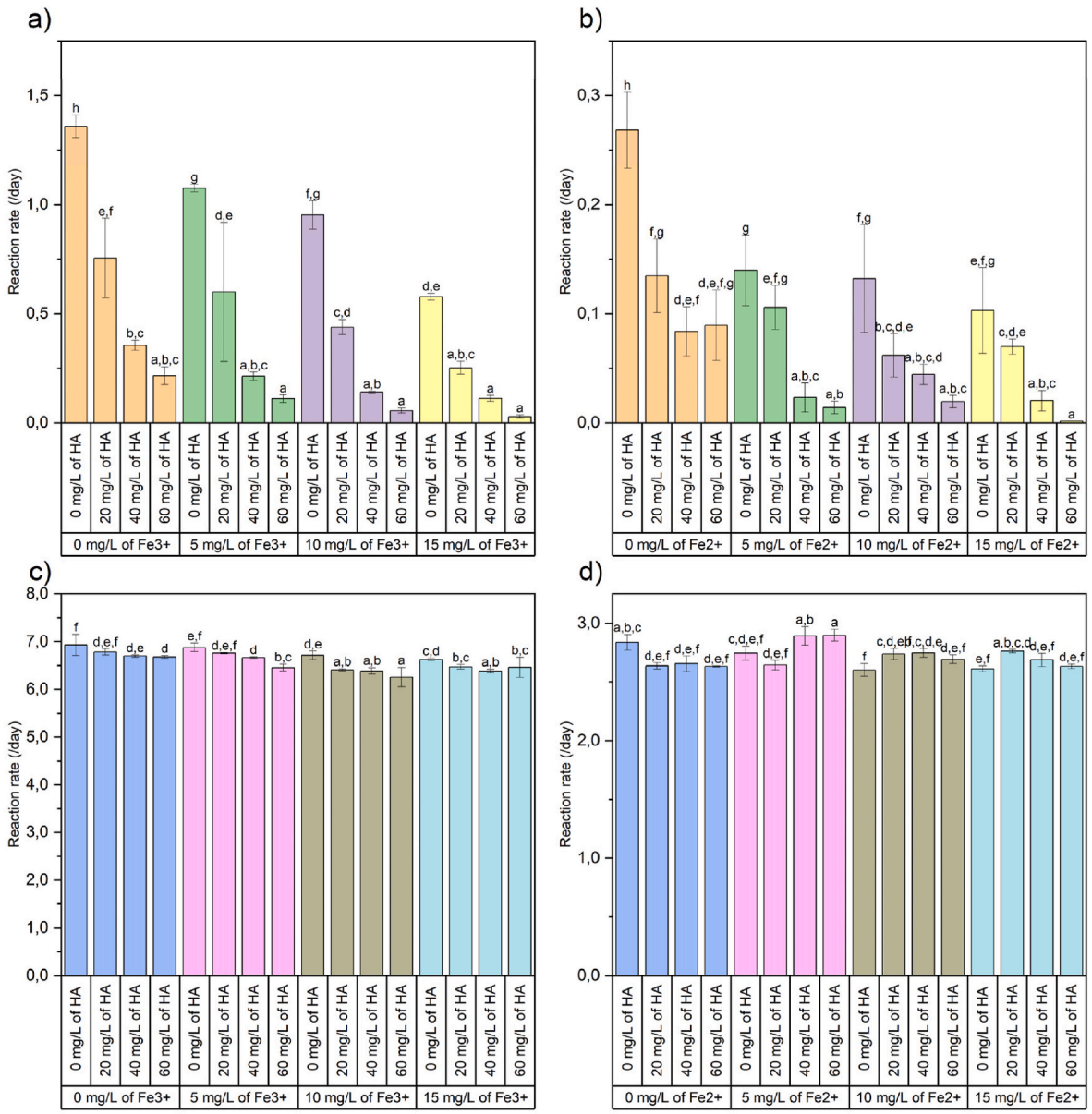

Fig. 1. Hydrolysis rate of (a–b) protein and (c–d) carbohydrate under aerobic (a, c) and anaerobic (b, d) conditions, respectively. The bar graphs represent the hydrolysis rate (mean ± SD). Different letters above the graph (a–h) indicate statistically significant differences in hydrolysis rate between variables based on ANOVA ($p \leq 0.05$), and variables sharing the same letter are not significantly different. The statistical analyses were conducted separately for aerobic and anaerobic conditions.

other organic groups (Pichtel et al., 1989) and HA can inhibit cellulose hydrolysis (Yap et al., 2018), which is in line with the slight inhibition observed in this study. Under anaerobic conditions (Fig. 1d), Fe(II) alone also reduced carbohydrate hydrolysis slightly (~5 %), but HA consistently inhibited hydrolysis across all concentrations. Interestingly, the combination of Fe(II) and HA sometimes alleviated inhibition, likely because HA preferentially complexed with Fe(II), leaving the substrate and enzyme more available to react (Fang et al., 2015). Nevertheless, at high concentrations (15 mg L^{-1} Fe(II) and 60 mg L^{-1} HA), the mixture again caused significant inhibition ($p < 0.05$).

Overall, hydrolysis rates were higher under aerobic than anaerobic conditions for both proteins and carbohydrates, consistent with previous reports that anaerobic hydrolysis is intrinsically slower (Podkaminer et al., 2012). These observations indicate that the extent of inhibition depends not only on the presence of Fe and HA but also on the prevailing redox conditions. The stability of the underlying complexes under different redox conditions is examined in Section 3.2.

3.2. Redox-dependent stability of Fe–protein–HA complexes

Distinct differences in protein hydrolysis were observed in the presence of Fe and HA under both aerobic and anaerobic conditions, indicating variations in Fe-protein-HA complexation and reflecting the role of Fe speciation in determining complex stability. To gain further insight into complex formation and stability, SEC-HPLC was used to determine complex size, while FTIR (section 3.3) provided information on molecular interactions.

As shown in the SEC-HPLC chromatograms (Fig. 2a), mixtures of protein and HA alone displayed distinct peaks, as indicated by enhanced peak broadening. In contrast, no detectable peaks were observed when Fe(III) was added, indicating more complex ternary Fe-protein-HA aggregates rather than exclusive competition. Thus, instead of one ligand displacing the other, Fe(III) facilitated strong bridging interactions, producing high-molecular-weight aggregates that were removed during sample filtration before measurement. This was supported by the

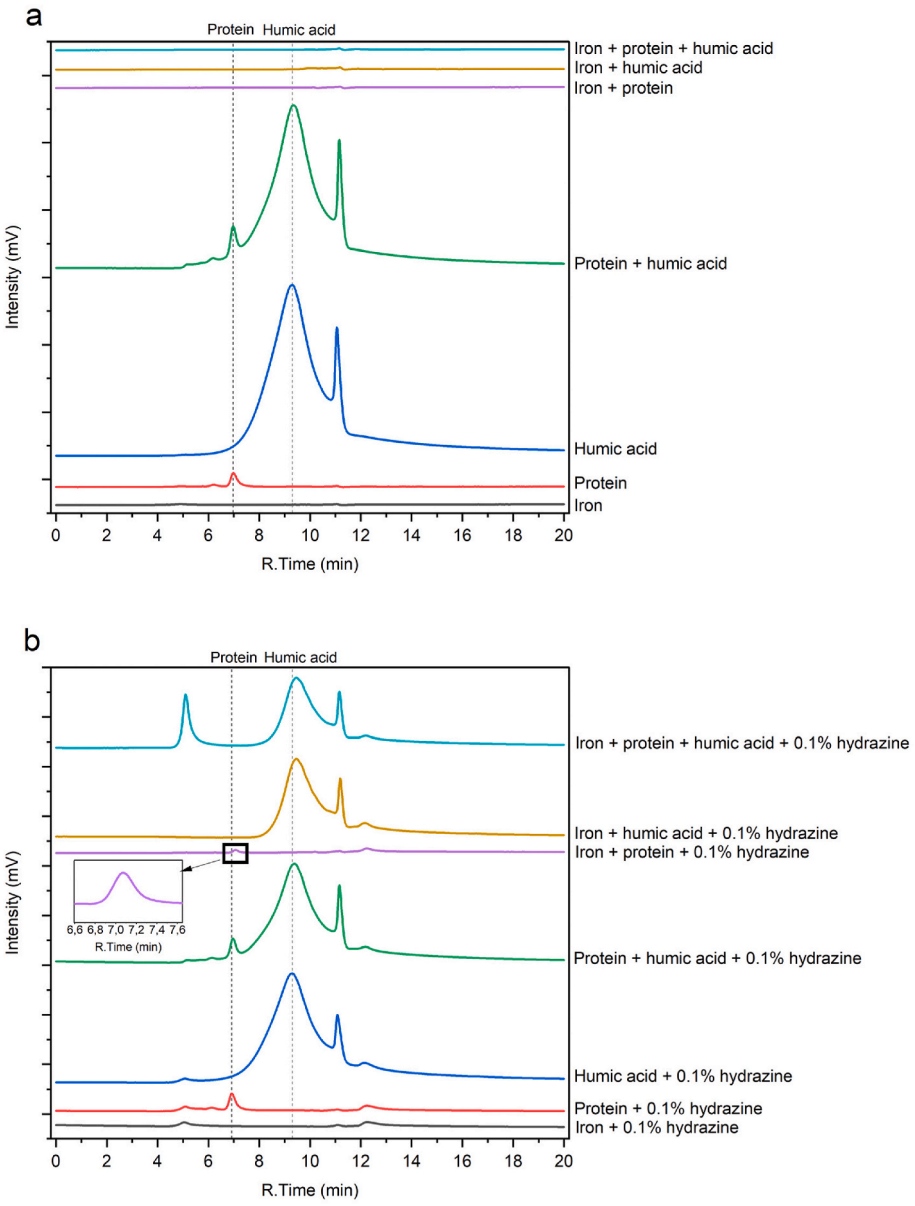

Fig. 2. SEC-HPLC results for complexation of protein–HA with 10 mg L^{-1} of Fe(III) under (a) aerobic and (b) anaerobic conditions.

measurements of free Fe(III) (Fig. 3a) that decreased from 7.3 ± 0.037 mg L^{-1} in the control to as low as 1.545 ± 0.001 mg L^{-1} when protein and HA were both present. Also free protein and HA (Fig. 3c and e) declined from 36 ± 0.35 and 135 ± 0.23 mg L^{-1} to 0 and 0 mg L^{-1}, respectively. Similar findings were reported by Boguta et al. (2019) and Permyakov (2021), Fe(III) promotes the aggregation of protein and HA into larger molecular-weight complexes with electrostatic and coordination bonds.

In contrast, under anaerobic conditions (Fig. 2b), where Fe was predominantly present as Fe(II) due to the conversion of Fe(III) by 0.1 % hydrazine, the protein and HA peaks remained visible at RT ~5 min and ~9.2 min, respectively. Moreover, the aggregates were eluted closer to their original retention times, indicating weaker and more reversible interactions. This observation is consistent with a previous study by Oh et al. (2015), which found that Fe(II), due to its lower charge density, forms less stable complexes and is less effective in bridging organic molecules. The free concentrations of Fe, protein, and HA (Fig. 3b, d, f) further support this interpretation: the free Fe concentration increased again to 7.3 ± 0.025 mg L^{-1} and the free HA concentration rose to 69.7 ± 9.42 mg L^{-1}, whereas free protein remained undetectable in the mixed solution. These results confirm that complexation was both weaker and more reversible under anaerobic than under aerobic conditions.

This trend was also observed at lower Fe concentrations (2.5 mg L^{-1}), as shown in the Supplementary Data (Fig. S1). The addition of Fe (III) to the mixed solution again produced earlier-eluting peaks (RT ~5 min) consistent with larger complexes, whereas Fe(II) led to peaks closer to those of the individual compounds. The consistency between 10 mg L^{-1} of Fe(III) and the supplementary experiment (2.5 mg L^{-1} of Fe(III)) demonstrates that the redox state of Fe, rather than its concentration, is the key determinant of complex stability. This finding aligns with previous studies, which have shown that both Fe(III) and Fe(II) form water-stable complexes with HA; however, Fe(III) generally occupies the most stable binding sites (Li et al., 2009, 2020).

Overall, these findings suggest that aerobic conditions favor strong Fe(III)-mediated bridging between proteins and HA, which significantly inhibits hydrolysis, whereas anaerobic conditions promote Fe(II) formation, leading to weaker interactions and increased substrate availability.

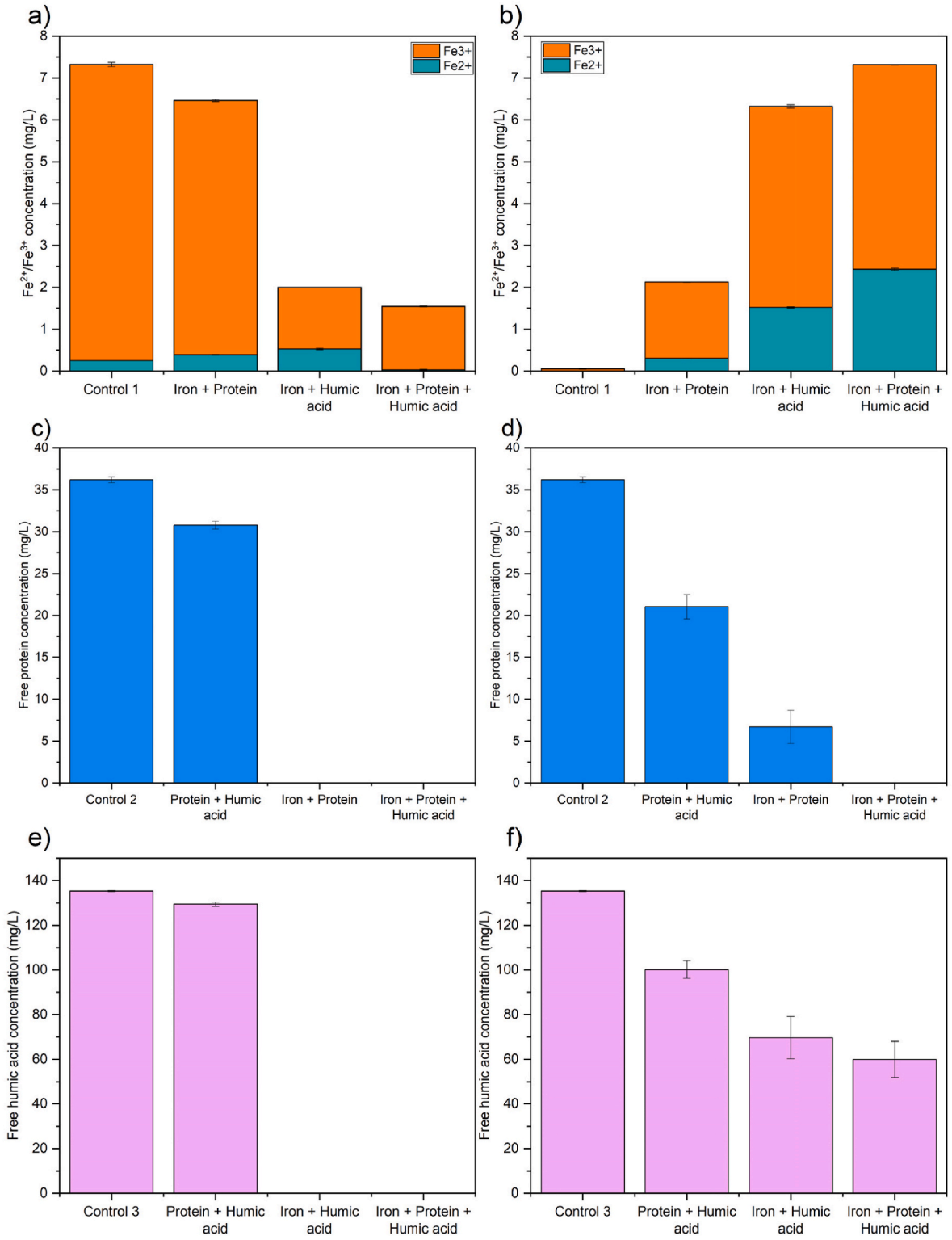

Fig. 3. (a–b) free iron, (c–d) free protein, and (e–f) free HA concentrations under aerobic (a, c, e) and anaerobic conditions (b, d, f), respectively.

3.3. Molecular interactions underlying Fe–protein–HA complexation

FTIR spectroscopy provided further insight into the molecular interactions between Fe(III), proteins, and HA observed under aerobic conditions. The spectra (Fig. 4) revealed clear shifts in characteristic bands of both protein and HA after the addition of Fe(III), indicating the involvement of specific functional groups in complexation. A detailed description of the different regions in the spectra is given in the supplementary data (Table S1 and S2).

Based on Fig. 4, the direct interaction of Fe(III) with peptide bonds of protein can be visualised by shifts in the Amide I (~1650 cm^{-1}) and II (~1550 cm^{-1}) regions. This interaction likely involves the oxygen atom of the C═O group and the nitrogen atom of the N–H group, forming stable protein-metal complexes (Lin et al., 2022). Changes and shifts in protein peaks can occur due to the presence of Fe, which is classified as a Lewis acid, allowing it to interact with functional groups in the protein

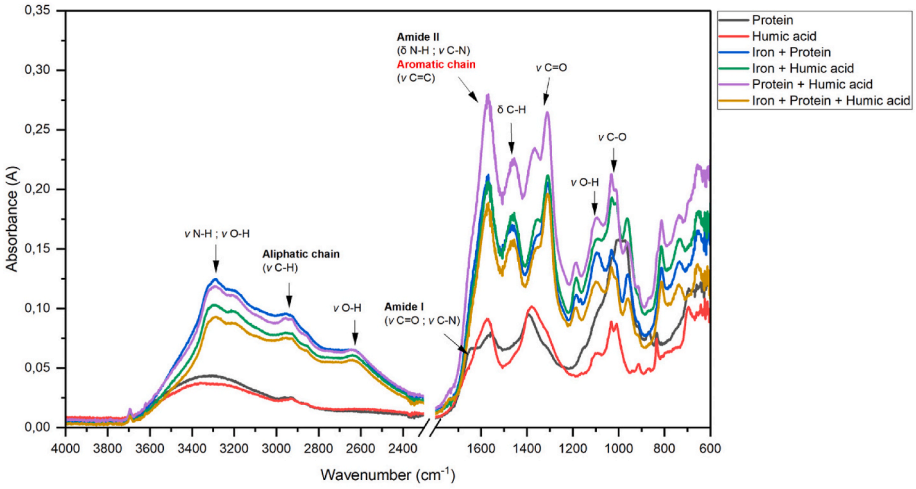

Fig. 4. FTIR results for the interaction of Fe(III) with functional groups of protein and HA.

by forming ligand bonds with electron-donating atoms such as nitrogen (amino groups) and oxygen (carboxyl or hydroxyl groups) (Ding et al., 2024). Fe(III) increased hydrogen bonding, indicated by the broadening of peaks in the 3300–3500 cm^{-1} range, possibly involving coordinated water molecules (Boguta et al., 2019). When Fe(III) interacts with HA, significant changes occur in the phenolic groups (~3000–3600 cm^{-1}) and aromatic groups (~1600 cm^{-1}), indicating strong interactions with these functional groups. The intensity of the aliphatic chain vibrations (~2900–2950 cm^{-1}) increased, suggesting greater rigidity or reduced flexibility of the aliphatic chains within the complex. This result is aligned with X. Li et al. (2020), who reported that these functional groups (phenolic groups, aliphatic groups, aromatic groups, and esters) play an important role in the complexation between Fe(III) with HA. Boguta et al. (2019) reported that the intensity of OH groups on HA increased after mixing with Fe(III), indicating their involvement in Fe-HA complexation through the formation of aqua ion complexes. Besides, the new peak at ~2632 cm^{-1} in the mixture is likely associated with O–H stretching vibrations in a strongly hydrogen-bonded environment (Barreto et al., 2020). Additional broadening and intensity changes observed in the 1200–1000 cm^{-1} region further supported the involvement of oxygen-containing groups, particularly the hydroxyl (–OH) and carboxyl (C═O) groups, in complexation with Fe(III). These spectral features suggest that Fe(III), acting as a bridging ion, coordinates with multiple C–O groups in both HA and proteins, thereby altering their vibrational modes (Andrade et al., 2019; Boguta et al., 2019; Chen et al., 2016). This study revealed that Fe forms complexes with proteins and HA through electrostatic and/or coordination bonds, interacting with various functional groups, including phenolic, amino, carboxyl, hydroxyl, aliphatic, aromatic groups, and esters.

Overall, the effects of Fe interaction with protein and humic acid under different redox conditions are summarized in Table 1.

3.4. Limitations of simple substrates and relevance for complex wastewater matrices

This study was conducted to elucidate the complex behaviour of various compounds in wastewater with iron under alternating anaerobic and aerobic conditions. Varying redox conditions are commonly encountered in wastewater treatment systems, such as the anaerobic selectors followed by aerobic zones in biological phosphate removing systems, anaerobic digesters or anaerobic side stream reactors to reduce the quantity of WAS.

Our results demonstrate that Fe complexation with protein and carbohydrate reduces the degradation rate, a phenomenon that may also occur in full-scale WWTPs. When complexes are formed under aerobic conditions, proteins and carbohydrates can be entrapped within the AS flocs. During WAS disposal, which typically occurs under anaerobic conditions, Fe-floc complexation will weaken due to the reduction of Fe (III) to Fe(II), resulting in the release of organic matter into solution and making it available for degradation. This finding is consistent with previous studies (Baek et al., 2014; Lin et al., 2017; Zhao et al., 2020), which suggests that Fe reduction in AD can promote floc disintegration and the dissolution of organic matter.

This study aimed to contribute to a deeper understanding of the role of iron in the sequestration of organic compounds and its impact on their bioavailability under alternating redox conditions in wastewater treatment systems. However, the experiments were conducted with simple substrates, which are casein and bovine serum albumin as proteins, resorufin-cellobioside as carbohydrate, and commercial humic acid, which might not fully represent the much more complex and heterogeneous mixture of organic matter, including polysaccharides, lipids, microbial products, surfactants, and xenobiotics, as well as competing inorganic ions (Sajid et al., 2022). These choices for a well-defined, but simpler composition in this study ensured reproducibility and allowed mechanistic insights into the interactions of proteins, HA, and Fe. This higher complexity in practice likely affects the strength and properties of the complexation formed (Li et al., 2023).

Despite these simplifications, the results obtained still provide important insights. These results demonstrate that protein degradation is significantly susceptible to inhibition compared with carbohydrates, highlighting proteins as critical contributors to persistent COD in wastewater systems and clear evidence that Fe(III) and Fe(II) form complexes with different stabilities, showing that redox cycling can modulate the degree of inhibition. These insights are transferable to more complex systems, where iron dosing and alternating aerobic–anaerobic conditions are already common practice in wastewater treatment (Ferrentino et al., 2023; Wu et al., 2015).

Future studies should extend this work to real wastewater matrices, where multiple organic and inorganic components can simultaneously interact with Fe and enzymes. Such studies would help quantify the extent to which the mechanisms identified in this study, which are protein hydrolysis inhibition, Fe-mediated interaction, and redox-dependent complex stability, are expressed in practice. Bridging the gap between simplified systems and complex wastewater is crucial for transferring theoretical understanding into practical strategies for enhancing biodegradability.

4. Conclusion

This research aimed to investigate the interaction of Fe with protein

Table 1
Effect of Fe interaction with protein and humic acid under different redox conditions.

Combinations				Observed effect
Fe species	Compounds	Reducing agent	Conditions	
Fe(III)	Protein	–	Aerobic	•Strong binding led to the formation of larger aggregates at ≥ 10 mg L^{-1} of Fe(III). •Reduced availability of protein by up to 100 %. •Reduced the concentration of free Fe by up to 12 %. •Decreased hydrolysis rate of protein up to 75 %.
Fe(III)	Humic acid	–	Aerobic	•In high concentrations (≥10 mg L^{-1}) of Fe(III), strong binding resulted in the formation of larger aggregates. •The availability of HA is reduced by up to 100 %. •Reduced free Fe concentration by up to 73 %.
Fe(III)	Protein and humic acid	–	Aerobic	•Strong binding resulted in the formation of larger aggregates at high concentrations (≥10 mg L^{-1}) of Fe(III). •Reduced availability of both compounds is up to 100 %. •Reduced the concentration of free Fe by up to 79 %. •Decreased hydrolysis rate of protein >90 %.
Fe(III)	Protein	Hydrazine	Anaerobic	•Weaker binding and reduced complexation. •Increased free protein concentrations to 18 %. •Convert Fe(III) to Fe(II) and Fe(0).
Fe(III)	Humic acid	Hydrazine	Anaerobic	•Weaker binding and lower complexation. •Increase free HA concentration up to 51 %. •Increase free Fe concentration up to 86 %. •Convert Fe(III) to Fe(II) and Fe(0).
Fe(III)	Protein and humic acid	Hydrazine	Anaerobic	•Weaker binding and lower complexation. •Protein is still in complex form. •Increase free HA concentration up to 44 %. •Increase free Fe concentration up to 100 %. •Convert Fe(III) to Fe(II).
Fe(II)	Protein	–	Anaerobic	•Weaker binding •Smaller aggregation. •Shifted protein peaks. •Decreased hydrolysis rate >50 %.
Fe(II)	Humic acid	–	Anaerobic	•Weaker binding •Smaller aggregation.
Fe(II)	Protein and humic acid	–	Anaerobic	•Weaker binding •Smaller aggregation. •Protein peaks shifted. •Decreased hydrolysis rate of protein >90 %.

and HA under different redox conditions. The results showed that under aerobic conditions, Fe(III) formed stable complexes with protein and HA, reducing the hydrolysis rates of protein by more than 90 %. These interactions resulted in larger molecular sizes and reduced protein availability, as determined by SEC-HPLC analysis. The FTIR analysis also confirmed that Fe(III) interacted with various functional groups of proteins and HA, including phenolic, amino, carboxyl, hydroxyl, aliphatic, and aromatic groups through electrostatic and/or coordination bonds, suggesting stable complex formations, as indicated by changes and shifts in the peaks. In contrast, under anaerobic conditions, the reduction of Fe(III) to Fe(II) significantly weakened the cross-links, leading to smaller complex sizes and increased dissolution of protein and HA. These findings highlight the significant role of Fe redox transformations in influencing protein-HA interactions and their availability. It is worth noting that this study employed simple substrates to facilitate controlled mechanistic analysis, whereas real wastewater comprises a much more complex mixture of organics and inorganics. Nevertheless, the identified results, such as protein hydrolysis inhibition, Fe-mediated interaction, and redox-dependent complex stability, are highly relevant for complex wastewater environments. These results provide a basis for future studies using real wastewater to validate and quantify these interactions under complex conditions.

CRediT authorship contribution statement

Muhammad Fauzul Imron: Writing – review & editing, Writing – original draft, Visualization, Validation, Methodology, Investigation, Formal analysis, Data curation, Conceptualization. **Lenno van den Berg:** Writing – review & editing, Validation, Supervision, Conceptualization. **Alexander T.W.M. Hendriks:** Writing – review & editing, Validation, Supervision, Methodology, Funding acquisition, Conceptualization. **Ralph E.F. Lindeboom:** Writing – review & editing, Validation, Supervision, Methodology, Funding acquisition, Conceptualization. **Merle K. de Kreuk:** Writing – review & editing, Validation, Supervision, Methodology, Funding acquisition, Conceptualization.

Declaration of competing interest

The authors declare that they have no known competing financial interests or personal relationships that could have appeared to influence the work reported in this paper.

Acknowledgment

The authors would like to thank the Indonesia Endowment Fund for Education (LPDP) and the Ministry of Finance of the Republic of Indonesia for funding the first author's PhD, as well as the Waterkracht collectief, which consists of Water Authorities Zuiderzeeland, Rijn en IJsel, Waterschap Vallei & Veluwe, Waterschap Vechtstromen and Waterschap Drents Overijsselse Delta, and Haskoning in The Netherlands, for supporting this research. Furthermore, the first author wishes to express his deepest appreciation to Javier Pavez-Jara for his guidance in operating the Fluorescence Microplate Reader and HPLC, and to Yuemei Lin for her invaluable assistance with the FTIR analysis. The lab staff of the TU Delft Waterlab is acknowledged for their analytical support.

Appendix A. Supplementary data

Supplementary data to this article can be found online at https://doi.org/10.1016/j.chemosphere.2025.144718.

Data availability

Data will be made available on request.

References

Aiken, G.R., Hsu-Kim, H., Ryan, J.N., 2011. Influence of dissolved organic matter on the environmental fate of metals, nanoparticles, and colloids. Environ. Sci. Technol. 45, 3196–3201. https://doi.org/10.1021/es103992s.

Andrade, J., Pereira, C.G., Almeida Junior, J.C. de, Viana, C.C.R., Neves, L.N. de O., Silva, P.H.F. da, Bell, M.J.V., Anjos, V. de C. dos, 2019. FTIR-ATR determination of protein content to evaluate whey protein concentrate adulteration. LWT 99, 166–172. https://doi.org/10.1016/j.lwt.2018.09.079.

Baek, G., Kim, J., Lee, C., 2014. Influence of ferric oxyhydroxide addition on biomethanation of waste activated sludge in a continuous reactor. Bioresour. Technol. 166, 596–601. https://doi.org/10.1016/j.biortech.2014.05.052.

Barreto, M.S.C., Elzinga, E.J., Alleoni, L.R.F., 2020. The molecular insights into protein adsorption on hematite surface disclosed by in-situ ATR-FTIR/2D-COS study. Sci. Rep. 10, 13441. https://doi.org/10.1038/s41598-020-70201-z.

Boguta, P., D'Orazio, V., Senesi, N., Sokołowska, Z., Szewczuk-Karpisz, K., 2019. Insight into the interaction mechanism of iron ions with soil humic acids: the effect of the pH and chemical properties of humic acids. J. Environ. Manage. 245, 367–374. https://doi.org/10.1016/j.jenvman.2019.05.098.

Catrouillet, C., Davranche, M., Dia, A., Bouhnik-Le Coz, M., Marsac, R., Pourret, O., Gruau, G., 2014. Geochemical modeling of Fe(II) binding to humic and fulvic acids. Chem. Geol. 372, 109–118. https://doi.org/10.1016/j.chemgeo.2014.02.019.

Chen, J., Zhong, L., Feng, H., Xie, Y., King, R.B., 2016. Bridging hydrogen atoms versus iron–iron multiple bonding in binuclear borole iron carbonyls. Inorganica Chim. Acta 447, 105–112. https://doi.org/10.1016/j.ica.2016.03.028.

Chen, R., Liu, H., Tong, M., Zhao, L., Zhang, P., Liu, D., Yuan, S., 2018. Impact of Fe(II) oxidation in the presence of iron-reducing bacteria on subsequent Fe(III) bio-reduction. Sci. Total Environ. 639, 1007–1014. https://doi.org/10.1016/j.scitotenv.2018.05.241.

Dampang, S., Purwanti, E., Destyorini, F., Kurniawan, S.B.K., Abdullah, S.R.S., Imron, M., 2021. Analysis of optimum temperature and calcination time in the production of CaO using seashells waste as CaCO3 source. J. Ecol. Eng. 22, 221–228. https://doi.org/10.12911/22998993/135316.

Di Iorio, E., Circelli, L., Angelico, R., Torrent, J., Tan, W., Colombo, C., 2022. Environmental implications of interaction between humic substances and iron oxide nanoparticles: a review. Chemosphere 303, 135172. https://doi.org/10.1016/j.chemosphere.2022.135172.

Ding, X., Liu, Y., Zheng, L., Chang, Q., Chen, X., Xi, C., 2024. Effect of different iron ratios on interaction and thermodynamic stability of bound whey protein isolate. Food Res. Int. 182, 114198. https://doi.org/10.1016/j.foodres.2024.114198.

Fang, K., Yuan, D., Zhang, L., Feng, L., Chen, Y., Wang, Y., 2015. Effect of environmental factors on the complexation of iron and humic acid. J. Environ. Sci. 27, 188–196. https://doi.org/10.1016/j.jes.2014.06.039.

Fernandes, T.V., van Lier, J.B., Zeeman, G., 2015. Humic acid-like and fulvic acid-like inhibition on the hydrolysis of cellulose and tributyrin. BioEnergy Res 8, 821–831. https://doi.org/10.1007/s12155-014-9564-z.

Ferrentino, R., Langone, M., Fiori, L., Andreottola, G., 2023. Full-scale sewage sludge reduction technologies: a review with a focus on energy consumption. Water 15, 615. https://doi.org/10.3390/w15040615.

Frølund, B., Griebe, T., Nielsen, P.H., 1995. Enzymatic activity in the activated-sludge floc matrix. Appl. Microbiol. Biotechnol. 43, 755–761. https://doi.org/10.1007/BF00164784.

Fujii, M., Imaoka, A., Yoshimura, C., Waite, T.D., 2014. Effects of molecular composition of natural organic matter on ferric iron complexation at circumneutral pH. Environ. Sci. Technol. 48, 4414–4424. https://doi.org/10.1021/es405496b.

Gonzalez, A., van Lier, J.B., de Kreuk, M.K., 2021. The role of growth media on composition, bioconversion and susceptibility for mild thermal pre-treatment of waste activated sludge. J. Environ. Manage. 298, 113491. https://doi.org/10.1016/j.jenvman.2021.113491.

Imron, M.F., Firdaus, A.A.F., Flowerainsyah, Z.O., Rosyidah, D., Fitriani, N., Kurniawan, S.B., Abdullah, S.R.S., Hasan, H.A., Wibowo, Y.G., 2023. Phytotechnology for domestic wastewater treatment: performance of pistia stratiotes in eradicating pollutants and future prospects. J. Water Process Eng. 51. https://doi.org/10.1016/j.jwpe.2022.103429.

Knap-Bałdyga, A., Żubrowska-Sudoł, M., 2023. Natural organic matter removal in surface water treatment via Coagulation—current issues, potential solutions, and new findings. Sustainability 15, 13853. https://doi.org/10.3390/su151813853.

Kügler, S., Cooper, R.E., Wegner, C.-E., Mohr, J.F., Wichard, T., Küsel, K., 2019. Iron-organic matter complexes accelerate microbial iron cycling in an iron-rich fen. Sci. Total Environ. 646, 972–988. https://doi.org/10.1016/j.scitotenv.2018.07.258.

Kurniawan, S.B., Imron, M.F., Abdullah, S.R.S., Othman, A.R., Hasan, H.A., 2023. Coagulation–flocculation of aquaculture effluent using biobased flocculant: from artificial to real wastewater optimization by response surface methodology. J. Water Process Eng. 53, 103869. https://doi.org/10.1016/j.jwpe.2023.103869.

Li, C., Fu, X., Qi, X., Hu, X., Chasteen, N.D., Zhao, G., 2009. Protein association and dissociation regulated by ferric ion. J. Biol. Chem. 284, 16743–16751. https://doi.org/10.1074/jbc.M109.011528.

Li, Q., Hu, W., Li, L., Li, Y., 2023. Interactions between organic matter and Fe oxides at soil micro-interfaces: quantification, associations, and influencing factors. Sci. Total Environ. 855, 158710. https://doi.org/10.1016/j.scitotenv.2022.158710.

Li, X., Wu, B., Zhang, Q., Liu, Y., Wang, J., Li, F., Ma, F., Gu, Q., 2020. Complexation of humic acid with Fe ions upon persulfate/ferrous oxidation: further insight from spectral analysis. J. Hazard. Mater. 399, 123071. https://doi.org/10.1016/j.jhazmat.2020.123071.

Lin, L., Li, R., Yang, Z., Li, X., 2017. Effect of coagulant on acidogenic fermentation of sludge from enhanced primary sedimentation for resource recovery: Comparison between FeCl 3 and PACl. Chem. Eng. J. 325, 681–689. https://doi.org/10.1016/j.cej.2017.05.130.

Lin, S., Hu, X., Yang, X., Chen, S., Wu, Y., Hao, S., Huang, H., Li, L., 2022. GLPGPSGEEGKR: Fe2+ chelating characterization and potential transport pathways for improving Fe2+ bioavailability in Caco-2 cells. Food Biosci. 48, 101806. https://doi.org/10.1016/j.fbio.2022.101806.

Maity, R., Chakraborty, D., Nandi, S., Yadav, A.K., Mullangi, D., Vinod, C.P., Vaidhyanathan, R., 2019. Aqueous-phase differentiation and speciation of Fe3+ and Fe2+ using water-stable photoluminescent lanthanide-based metal–organic framework. ACS Appl. Nano Mater. 2, 5169–5178. https://doi.org/10.1021/acsanm.9b01047.

Mbamalu Ezeh, E., Chinedu Agu, P., Aworabhi, E., 2024. Biological treatment techniques for sewage: aerobic and anaerobic processes. In: Sewage - Management and Treatment Techniques. IntechOpen. https://doi.org/10.5772/intechopen.1006097.

Mittal, V.A., Ellis, A., Ye, A., Das, S., Singh, H., 2015. Influence of calcium depletion on iron-binding properties of milk. J. Dairy Sci. 98, 2103–2113. https://doi.org/10.3168/jds.2014-8474.

Mundra, S., Tits, J., Wieland, E., Angst, U.M., 2023. Aerobic and anaerobic oxidation of ferrous ions in near-neutral solutions. Chemosphere 335, 138955. https://doi.org/10.1016/j.chemosphere.2023.138955.

Oh, I., Kim, M., Kim, J., 2015. Controlling hydrazine reduction to deposit iron oxides on oxidized activated carbon for supercapacitor application. Energy 86, 292–299. https://doi.org/10.1016/j.energy.2015.04.040.

Permyakov, E.A., 2021. Metal binding proteins. Encyclopedia 1, 261–292. https://doi.org/10.3390/encyclopedia1010024.

Pichtel, J.R., Dick, W.A., McCoy, E.L., 1989. Binding of iron from pyritic mine spoil by water-soluble organic materials extracted from sewage sludge. Soil Sci. 148, 140–148. https://doi.org/10.1097/00010694-198908000-00008.

Podkaminer, K.K., Kenealy, W.R., Herring, C.D., Hogsett, D.A., Lynd, L.R., 2012. Ethanol and anaerobic conditions reversibly inhibit commercial cellulase activity in thermophilic simultaneous saccharification and fermentation (tSSF). Biotechnol. Biofuels 5, 43. https://doi.org/10.1186/1754-6834-5-43.

Qasem, N.A.A., Mohammed, R.H., Lawal, D.U., 2021. Removal of heavy metal ions from wastewater: a comprehensive and critical review. npj Clean Water 4, 36. https://doi.org/10.1038/s41545-021-00127-0.

Sajid, M., Asif, M., Baig, N., Kabeer, M., Ihsanullah, I., Mohammad, A.W., 2022. Carbon nanotubes-based adsorbents: properties, functionalization, interaction mechanisms, and applications in water purification. J. Water Process Eng. 47, 102815. https://doi.org/10.1016/j.jwpe.2022.102815.

Steinhauser, S., Heinz, U., Bartholomä, M., Weyhermüller, T., Nick, H., Hegetschweiler, K., 2004. Complex formation of ICL670 and related ligands with Fe III and Fe II. Eur. J. Inorg. Chem. 4177–4192. https://doi.org/10.1002/ejic.200400363, 2004.

Wu, H., Ikeda-Ohno, A., Wang, Y., Waite, T.D., 2015. Iron and phosphorus speciation in Fe-conditioned membrane bioreactor activated sludge. Water Res. 76, 213–226. https://doi.org/10.1016/j.watres.2015.02.020.

Yang, G., Zhang, P., Zhang, G., Wang, Y., Yang, A., 2015. Degradation properties of protein and carbohydrate during sludge anaerobic digestion. Bioresour. Technol. 192, 126–130. https://doi.org/10.1016/j.biortech.2015.05.076.

Yap, S.D., Astals, S., Lu, Y., Peces, M., Jensen, P.D., Batstone, D.J., Tait, S., 2018. Humic acid inhibition of hydrolysis and methanogenesis with different anaerobic inocula. Waste Manag. 80, 130–136. https://doi.org/10.1016/j.wasman.2018.09.001.

Zhan, W., Tian, Y., Zhang, J., Zuo, W., Li, L., Jin, Y., Lei, Y., Xie, A., Zhang, X., 2021. Mechanistic insights into the roles of ferric chloride on methane production in anaerobic digestion of waste activated sludge. J. Clean. Prod. 296, 126527. https://doi.org/10.1016/j.jclepro.2021.126527.

Zhao, Zisheng, Li, Y., Zhao, Zhiqiang, Yu, Q., Zhang, Y., 2020. Effects of dissimilatory iron reduction on acetate production from the anaerobic fermentation of waste activated sludge under alkaline conditions. Environ. Res. 182, 109045. https://doi.org/10.1016/j.envres.2019.109045.

Zhu, G., Zheng, H., Zhang, Z., Tshukudu, T., Zhang, P., Xiang, X., 2011. Characterization and coagulation–flocculation behavior of polymeric aluminum ferric sulfate (PAFS). Chem. Eng. J. 178, 50–59. https://doi.org/10.1016/j.cej.2011.10.008.

Zhu, X., Liu, J., Li, L., Zhen, G., Lu, X., Zhang, J., Liu, H., Zhou, Z., Wu, Z., Zhang, X., 2023. Prospects for humic acids treatment and recovery in wastewater: a review. Chemosphere 312, 137193. https://doi.org/10.1016/j.chemosphere.2022.137193.